Heat management of thermally coupled reactors for conducting simultaneous endothermic and exothermic reactions

Junjie Chen

Department of Energy and Power Engineering, School of Mechanical and Power Engineering, Henan Polytechnic University, Jiaozuo, Henan, 454000, P.R. China

* Corresponding author, E-mail address: cjjtpj@163.com, https://orcid.org/0000-0002-4222-1798

Abstract

Computational fluid dynamics simulations are carried out to better understand how to manage thermally coupled reactors for conducting simultaneous endothermic and exothermic reactions. Particular emphasis is placed upon the mechanisms involved in the heat transfer processes in thermally coupled reactors for hydrogen production by steam reforming. The effects of catalyst layer thickness on the enthalpy of reaction, methanol conversion, and hydrogen yield are delineated. The oxidation and reforming reaction rates involved in the endothermic and exothermic processes are determined. Contour maps denoting temperature, enthalpy, and species mole fractions are constructed and design recommendations are made. The results indicate that the waste heat can efficiently be recovered in a low-temperature region, although the reactivity of a steam reforming reaction is low in such a region. The steam reforming device is configured as to be heated by part of the combustion heat to cause a steam reforming reaction in the device. The steam reforming reaction is endothermic and is therefore typically carried out in an externally heated steam reforming reactor. The incorporation of a simultaneous exothermic reaction to provide an improved heat source can provide a typical heat flux of roughly an order of magnitude above the convective heat flux. Structured catalysts offer heat transfer benefits and extra activity, which is more effective in the inlet zone of the steam reformer. The metallic support is formed substantially to have the same shape as the reactor wall and is arranged in a direct heat conduction relationship with the reactor wall. Desirably all of the tubes contain the same proportions of structured catalyst and particulate catalyst, which provides the benefits of the higher activity, higher heat transfer, and low pressure drop of the structured catalyst at the inlet end and the benefit of the stronger particulate catalyst at the outlet end. Heat transport is more efficient when catalyzed hardware is used in the steam reforming process.

Keywords: Heat transfer; Heat management; Heat fluxes; Heat losses; Heat resistances; Heat exchange

1. Introduction

Chemical reactors are devices or vessels within which chemical processes are carried out for experimental or manufacturing purposes [1, 2]. The preparation of many industrially important chemicals by reversible reactions, for example, the production of hydrogen by steam reforming, is limited by reaction rates that are relatively low under conditions of favorable equilibrium [3, 4]. A number of measures have been devised for the purpose of creating more favorable equilibrium conditions, in order to increase reaction rates and hence productivity for a particular reaction [5, 6]. In the case of the production of hydrogen by steam reforming, for example, the disadvantage of the relatively low equilibrium constant at normal pressures, for the temperatures at which the reaction takes place, may be overcome by the use of increased pressure to the steam-hydrogen equilibrium, resulting in increased productivity of hydrogen [7, 8]. The presence of a catalyst in other cases, for example, in the production of sulfur trioxide from sulfur dioxide and oxygen, permits the use of a lower, more

advantageous temperature by shortening the time needed to establish equilibrium consequently resulting in shorter reaction times and increased productivity.

For every equilibrium reaction in which the reverse reaction is favored by high temperatures, there is some intermediate temperature at which the forward production rate and equilibrium reconversion can be balanced to give an optimum design for the forward reaction in an isothermal reactor system [9, 10]. If temperature is controlled to vary with time, an optimum heat-up and cool-down cycle for this system exists [11, 12]. For such a cycle, heat is supplied or removed uniformly to or from the reactor contents, so that the temperature change of the reactor contents is progressively isothermal, or in other words, is substantially uniform throughout the reactor at a given time [13, 14]. This is conventionally accomplished by heating the reactor and contents uniformly, or by heating the reactor and stirring the contents thereof [15, 16]. The temperature differential or gradient consequently imposed, is in respect of time only, referred to as a time-temperature gradient. The optimum time-temperature relation for a slug of gas in a well-designed sulfur dioxide converter, for example, calls for an increase in temperature in the early stage, to maximize the reaction rate, followed by a decrease in temperature in the final stage, to take advantage of more favorable equilibrium conversions at the lower temperatures [17, 18]. When pressure has an influence on the ratio of the fugacity coefficients for the components of an equilibrium reaction, or when there is a change in the total number of moles of products as compared with the total number of moles of reactants; it can be expected that the production capacity of a reactor unit will vary with the pressure [19, 20]. The usual way of coping with the situation is to predetermine and fix the pressure of such a reaction at a practical and advantageous level and carry out the reaction according to the optimum time-temperature cycle, which can be determined by standard techniques.

The production capacities of such systems can be increases considerably and in some cases by as much as 100 percent over those capacities obtained by using the optimum time-temperature cycle, by heating the reactor and contents to reaction temperatures and above, non-uniformly, so that two or more zones of unequal temperatures are created throughout the reactor [21, 22]. The temperature differential or gradient consequently imposed is in respect of position in the reactor, as well as time, referred to as a time-position-temperature gradient. The cooler portion or portions of the reactor prevent dissociation of the product and excessive pressure build-up, while permitting a higher reaction rate in the warmer portion or portions of the reactor than would otherwise be obtainable [23, 24]. Moreover, the increased density of the gaseous components within the cooler portion or zones of the reactor permits larger charges of reactants to be made and stored within the reactor, without the accompanying disadvantage of over-pressurization [25, 26]. The over-all result is an increase in productivity of the reactor, or in other words, more pounds per hour of sought-for product [27, 28]. It is accordingly necessary to provide a means for increasing productivity of chemical reactors in equilibrium reactions wherein the forward reaction is favored by conditions of high pressure. It is further necessary to provide a means for increasing the productivity of a chemical reactor in equilibrium reactions wherein the total number of moles of product components is less than the total number of moles of reactant components. It is also necessary to provide a means for increasing the productivity of a high-pressure chemical reactor in equilibrium reactions wherein the compressibility of the products is greater than the compressibility of the reactants. It is very necessary to provide a means for increasing the productivity of a chemical reactor used for producing hydrogen by steam reforming.

The present study is focused primarily upon the heat management of thermally coupled reactors for conducting simultaneous endothermic and exothermic reactions. Computational fluid dynamics simulations are carried out to better understand how to manage thermally coupled reactors for conducting simultaneous endothermic and exothermic reactions. Thermally coupled reactors are used for conducting simultaneous endothermic and exothermic chemical reactions. The endothermic reaction may be conducted in the one or more process layers and may comprise a steam reforming reaction. The

exothermic reaction may be conducted in the one or more heat exchange layers and may comprise a combustion reaction or a partial oxidation reaction. Exothermic heat may transfer from the one or more heat exchange layers to the one or more process layers. When more than one process layer and more than one heat exchange layer are used, they may be aligned in alternating sequence, or two or more process layers and two or more heat exchange layers may be positioned adjacent to each other. The present study aims to provide a fundamental understanding of the mechanisms of how to manage thermally coupled reactors for conducting simultaneous endothermic and exothermic reactions. Particular emphasis is placed upon the mechanisms involved in the heat transfer processes in thermally coupled reactors for hydrogen production by steam reforming.

2. Methods

An integrated parallel plate microreactor configuration is simulated. The oxidation and reforming reactions are carried out in alternate channels separated by walls. The stoichiometric methanol-air flow in the oxidation channel is co-current with respect to the methanol-steam flow in the reforming channel. Both the fluid streams enter the device at room temperature and exit at atmospheric pressure. Using the inherent symmetry of the geometry, only one-half of each channel and the connecting wall are simulated. The fluid flow as well as the heat and mass transfer equations are solved in the fluid phase and the energy balance is explicitly accounted for in the solid wall. A steady-state solution of the problem is sought using computational fluid dynamics. More specifically, computational fluid dynamics is used to solve the steady-state continuity, momentum, energy, and species conservation equations in the fluid phase and the heat equation in the solid phase using a finite volume approach. An adaptive meshing scheme is used for the discretization of the differential equations. The computational mesh is initialized with 200 axial nodes, 200 radial nodes for the oxidation channel and the wall sections, and 200 radial nodes for the reforming channel. This discretization translates into a total of about 80000 nodes. This initial mesh is adapted and refined during a calculation to increase the accuracy of the solution in regions of high gradients. Specifically, additional nodes are introduced to refine the mesh using the tools built in the computational software. Specifically, mesh refinement before achieving complete convergence reduces the computational effort, but a too early refinement, namely in a few iterations, may lead to refinement in wrong regions. Such an adaptive meshing strategy, starting with a relatively coarse initial mesh followed by refinement in regions of large gradients, achieves an adequate balance between accuracy and computational effort.

The fluid density is calculated using the ideal gas law. The individual properties of various gaseous species, such as thermal conductivity, are calculated using the kinetic theory of gases, whereas the specific heats are determined as a function of temperature using polynomial fits from the thermodynamic database. Mixture properties, such as specific heat and thermal conductivity, are calculated from pure component values based on the mass-fraction weighted mixing law. Binary species diffusivities are determined and then are used to calculate the multicomponent mixture diffusivities. For the solid wall, a constant specific heat and an isotropic thermal conductivity are specified. Given that material conductivity varies with temperature and more importantly with the material chosen, simulations are carried out over a wide range of conductivities. To permit modeling of fluid flow and related transport phenomena in industrial equipment and processes, various useful features are provided. These include porous media, lumped parameter streamwise-periodic flow and heat transfer, swirl, and moving reference frame models. The moving reference frame family of models includes the ability to model single or multiple reference frames. A time-accurate sliding mesh method, useful for modeling multiple stages in turbomachinery applications, for example, is also provided, along with the mixing plane model for computing time-averaged flow fields. Another very useful group of models is the set of free surface and multiphase flow models. These can be used for analysis of

gas-liquid, gas-solid, liquid-solid, and gas-liquid-solid flows. For all flows, conservation equations for mass and momentum are solved. For flows involving heat transfer or compressibility, an additional equation for energy conservation is solved. For flows involving species mixing or reactions, a species conservation equation is solved or, if the non-premixed combustion model is used, conservation equations for the mixture fraction and its variance are solved. Additional transport equations are also solved when the flow is turbulent.

The flow of thermal energy from matter occupying one region in space to matter occupying a different region in space is known as heat transfer [29, 30]. Heat transfer can occur by three main methods: conduction, convection, and radiation. The net transport of energy at inlets consists of both the convection and diffusion components. The convection component is fixed by the inlet temperature specified. The diffusion component, however, depends on the gradient of the computed temperature field [31, 32]. Consequently, the diffusion component and therefore the net inlet transport is not specified a priori. When heat is added to a fluid and the fluid density varies with temperature, a flow can be induced due to the force of gravity acting on the density variations. Such buoyancy-driven flows are termed natural-convection or mixed-convection flows. Multiple simultaneous chemical reactions can be modeled, with reactions occurring in the bulk phase and on wall surfaces, and in the porous region [33, 34]. For gas-phase reactions, the reaction rate is defined on a volumetric basis and the rate of creation and destruction of chemical species becomes a source term in the species conservation equations. For surface reactions, the rate of adsorption and desorption is governed by both chemical kinetics and diffusion to and from the surface [35, 36]. Wall surface reactions consequently create sources and sinks of chemical species in the gas phase, as well as on the reacting surface. Reactions at surfaces change gas-phase, surface-adsorbed and bulk species. On reacting surfaces, the mass flux of each gas specie due to diffusion and convection to and from the surface is balanced with its rate of consumption and production on the surface. The model boundary conditions are described next. Boundary conditions consist of flow inlets and exit boundaries and wall boundaries. Symmetry boundary conditions are used since the physical geometry of interest, and the expected pattern of the flow and thermal solution, have mirror symmetry. The axis boundary type is used as the centerline of an axisymmetric geometry. Both gases enter the channels at room temperature with a uniform, flat flow velocity. The reactor exits are held at a fixed pressure and the normal gradients of species and temperature, with respect to the direction of the flow, are set to zero. Symmetry boundary condition is applied at the centerline of both channels, implying a zero normal velocity and zero normal gradients of all variables. No-slip boundary condition is applied at each wall-fluid interface. Overall, the device is adiabatic, namely no heat losses occur through the side walls. Continuity in temperature and heat flux is applied at the fluid-solid interfaces. Neither heat-transfer nor mass-transfer correlations are employed since detailed transport within the solid and fluid phases is explicitly accounted for.

The pressure-based solver traditionally has been used for incompressible and mildly compressible flows [37, 38]. The density-based approach, on the other hand, is originally designed for high-speed compressible flows [39, 40]. Both approaches are now applicable to a broad range of flows, from incompressible to highly compressible, but the origins of the density-based formulation may give it an accuracy, namely shock resolution, advantage over the pressure-based solver for high-speed compressible flows [41, 42]. Two formulations exist under the density-based solver: implicit and explicit. The density-based explicit and implicit formulations solve the equations for additional scalars, for example, turbulence or radiation quantities, sequentially [43, 44]. The implicit and explicit density-based formulations differ in the way that they linearize the coupled equations. In both methods the velocity field is obtained from the momentum equations [45, 46]. In the density-based approach, the continuity equation is used to obtain the density field while the pressure field is determined from the equation of state. On the other hand, in the pressure-based approach, the pressure field is extracted by

solving a pressure or pressure correction equation which is obtained by manipulating continuity and momentum equations. In both cases a control-volume-based technique is used that consists of division of the domain into discrete control volumes using a computational grid, integration of the governing equations on the individual control volumes to construct algebraic equations for the discrete dependent variables, such as velocities, pressure, temperature, and conserved scalars, and linearization of the discretized equations and solution of the resultant linear equation system to yield updated values of the dependent variables. The two numerical methods employ a similar discretization process, but the approach used to linearize and solve the discretized equations is different. The full computational fluid dynamics problem is solved via a segregated solver using an under-relaxation method. Convergence of the solution is monitored through the residuals of the governing equations and the norm of successive iterations of the solution. The coupling of the heat equation in the wall and the reacting flow equations makes the problem stiff due to the disparity in thermal conductivity between the gases and the wall. Typical computational fluid dynamics simulation times varies from about several hours to a few days on a single processor depending on the stiffness of the problem. Natural parameter continuation is employed to study the effect of various operating parameters.

3. Results and discussion

The hydrogen mole fraction and temperature contour plots are illustrated in Figure 1 in the thermally coupled reactor for conducting simultaneous endothermic and exothermic reactions. Heating with part of the combustion heat may be carried out by direct heating or radiation heating. Accordingly, the waste heat can efficiently be recovered in a low-temperature region, although the reactivity of a steam reforming reaction is low in such a low-temperature region, because a reforming catalyst effectively acts. The waste heat can also efficiently be recovered even in the absence of a steam reforming catalyst in a high-temperature region because the reactivity of a steam reforming reaction is high in such a high-temperature region. In this connection, metal tubular reactors have insufficient thermal stability. For example, a metal material has significantly decreased strength at temperatures higher than 800 °C and has strength of about 100 MPa at 1000 °C. Accordingly, an actual steam reforming apparatus must operate at a controlled operation temperature of about 200 °C to about 300 °C. The temperature of 300 °C refers to temperature at which such a metal tubular reactor can be used, and, if a metal tubular reactor is continuously operated at temperatures above 300 °C, it may possibly be broken due to decreased strength thereof. At a temperature equal to or lower than the temperature where a metal tubular reactor can be used, the conversion decreases when no catalyst is used, and therefore a catalyst should essentially be used to compensate the decrease in conversion. Accordingly, ceramic materials can be used as tubular reactors even at temperatures of 1000 °C or higher where it is impossible to use metal materials. In contrast, there is no need of using a steam reforming catalyst at temperatures of 1000 °C or higher, because the conversion is complete even in the absence of a catalyst at temperatures of 1000 °C or higher. In addition, it is difficult to use a steam reforming catalyst at such high temperatures. A steam reforming catalyst generally includes catalytic metal nickel particles dispersed on an alumina carrier, and the nickel particles gradually undergo sintering and become coarse at temperatures of 1000 °C or higher. Such coarse nickel particles have reduced specific surface areas and show decreased reactivity. That is, steam reforming catalysts generally have heat resistance up to at a temperature of about 1000° C, and it is impossible to use such catalysts at temperatures of 1000 °C or higher, while the heat resistance somewhat varies depending on the type of a metal. Thus, steam reforming can be carried out even at temperatures of 1000 °C or higher by using a ceramic tube, whereas metal tubular reactors and catalysts cannot be used at such high temperatures. The thermally coupled reactor can thereby recover waste heat effectively, and can carry out a steam reforming reaction even in a region at high temperatures.

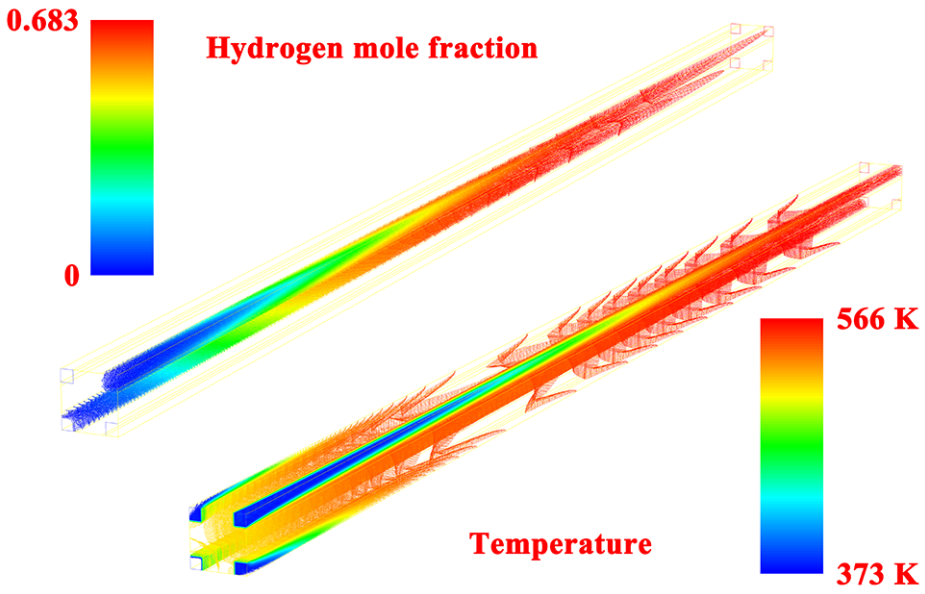

Figure 1. Hydrogen mole fraction and temperature contour plots in the thermally coupled reactor for conducting simultaneous endothermic and exothermic reactions.

The steam and carbon dioxide mole fraction contour plots are illustrated in Figure 2 in the thermally coupled reactor for conducting simultaneous endothermic and exothermic reactions. When a combustion furnace for burning methanol to be heated is used as an industrial furnace, ceramic tubular reactors are preferably used both in a high-temperature reforming section and in a low-temperature reforming section. When an industrial furnace is a combustion furnace, gases in the industrial furnace and an exhaust gas from the industrial furnace may contain various corrosive components. These components are generally rendered harmless after being discharged from the furnace and are emitted. On the other hand, heat is preferably recovered in the furnace or immediately after discharging from the furnace so as to recover and use the energy of waste heat more efficiently. A tubular reactor, if arranged in an atmosphere containing corrosive components, must include a corrosion-resistant material [47, 48]. Metals may not be used due to corrosion even at temperatures lower than their allowable temperature limits under some conditions upon use [49, 50]. Some ceramics, however, can be used even under such severe conditions. Consequently, steam reforming can be carried out, and the waste heat of the furnace can be effectively used under conditions where metal tubular reactors are not usable even at temperatures lower than 300 °C. This can be achieved by using a ceramic tubular reactor made from a ceramic material in accordance with a contained corrosive component. When a kiln is used as an industrial furnace, a low-temperature reforming section preferably includes a metal tubular reactor in view of economic efficiency, but it may include a ceramic tubular reactor. Even if a kiln is used as an industrial furnace, the low-temperature reforming section preferably includes a ceramic tubular reactor when an atmosphere in the low-temperature reforming section may cause corrosion. The sizes and numbers of metal tubular reactors and ceramic tubular reactors can be set as appropriate according to the size of the kiln, the amount of the combustion gas, the temperature of the combustion gas, and locations of the tubular reactors. Such tubular reactors may have a simple cylindrical form but may also have, for example, protrusions or blades on their outer surface. The resulting tubular reactors have increased heat-receiving areas and thereby receive increased heat per unit length of the reforming tubes. In addition, a shape having the length necessary for a predetermined reaction quantity may be employed. Accordingly, the waste heat can efficiently be recovered in a location at temperatures of 600 °C or higher and lower than 1000 °C, although the reactivity of a steam reforming reaction is low in such a low-temperature region, because a reforming catalyst effectively acts. The waste heat can also efficiently be recovered even in the absence of a reforming catalyst in a location at temperatures of

1000 °C or higher and 1800 °C or lower because the reactivity of a steam reforming reaction is high in such a high-temperature region. In addition, the advantages obtained by using the steam reforming apparatus can be obtained. The steam reforming apparatus in the kiln is configured as to be heated by part of the combustion heat to cause a steam reforming reaction as in the steam reforming apparatus. The part of the combustion heat herein includes a directly received heat and a radiant-heat-derived heat. Specifically, the combustion gas comes in direct contact with a metal tubular reactor and a ceramic tubular reactor to give heat to the metal tubular reactor and the ceramic tubular reactor.

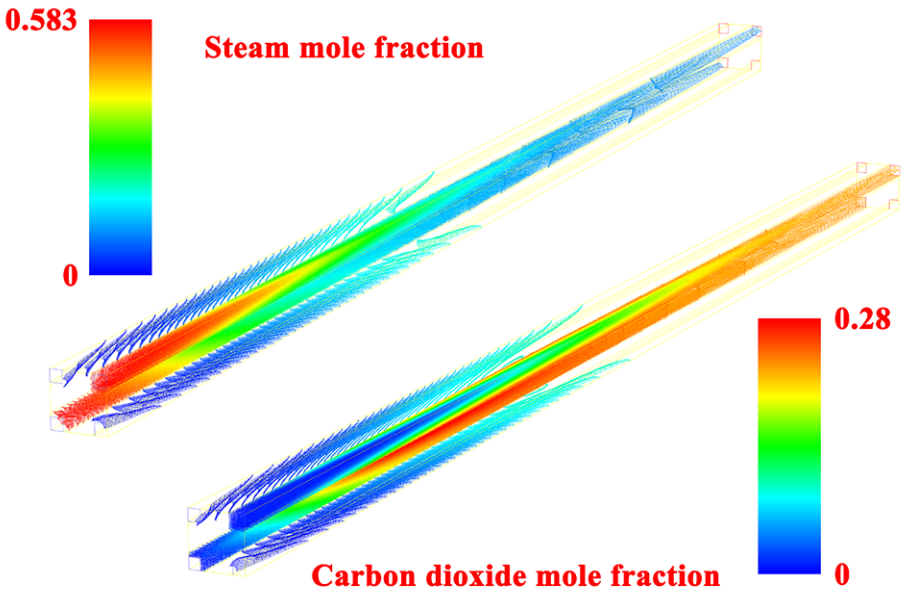

Figure 2. Steam and carbon dioxide mole fraction contour plots in the thermally coupled reactor for conducting simultaneous endothermic and exothermic reactions.

The effect of catalyst layer thickness on the enthalpy of reaction in the oxidation and reforming processes is illustrated in Figure 3 in the thermally coupled reactor for conducting simultaneous endothermic and exothermic reactions. The steam reforming reaction is endothermic and is therefore typically carried out in an externally heated steam reforming reactor, usually a multi-tubular steam reformer comprising a plurality of parallel tubes placed in a furnace, each tube containing a fixed bed of steam reforming catalyst particles. The feedstock is typically first pre-heated, usually in heat exchange contact with flue gas from the burners of the furnace, before it is supplied to the catalyst-filled tubes. In catalytic steam reforming processes, fouling of the catalyst bed by coke formation is a major problem. Typically, at temperatures above 400 or 450 °C, carbon-containing deposits are formed on metal catalysts in the presence of hydrocarbons and carbon monoxide. Such carbon deposits result in for example pressure drop problems and reduced catalyst activity due to covering of active catalyst sites. When oxygenated hydro-carbonaceous feedstocks are used, the coke formation problem is more pronounced, since oxygenated hydro-carbonaceous feedstocks are more thermo-labile than hydrocarbons and therefore more prone to carbon formation. In steam reforming processes, the deactivated or spent catalyst is typically regenerated by burning off the carbon in a separate burner or by oxidizing the carbon by supplying steam to the reforming zone whilst stopping the supply of the feedstock. During a first period of time a feedstock comprising an oxygenated hydrocarbon and a hydrocarbon is converted into synthesis gas by contacting the feedstock and steam with a steam reforming catalyst. During the first period, oxygenated hydrocarbon, hydrocarbon and steam are supplied to the steam reforming catalyst under steam reforming conditions. As a result, synthesis gas is formed and the catalyst will gradually become deactivated due to deposition of carbon on the catalyst. Consequently, deactivated steam reforming catalyst is obtained during the first period of time. During a second period of time, consecutive to the first period of time, namely directly

following the first period, the deactivated reforming catalyst is regenerated. The regeneration is carried out by stopping the supply of oxygenated hydrocarbon to the catalyst whilst the supply of hydrocarbon and steam is maintained. Also, the regeneration is carried out under steam reforming operating conditions. After the second period of time, namely the regeneration, the catalyst activity will be increased, typically to a level approaching the original catalyst activity, and the supply of oxygenated hydrocarbon is typically resumed. Another sequence of first period with supply of oxygenated hydrocarbon and second period wherein the supply of oxygenated hydrocarbon is stopped will then typically be carried out. The steam reforming process is preferably carried out in the absence of a molecular-oxygen containing gas both during the first and during the second period of time.

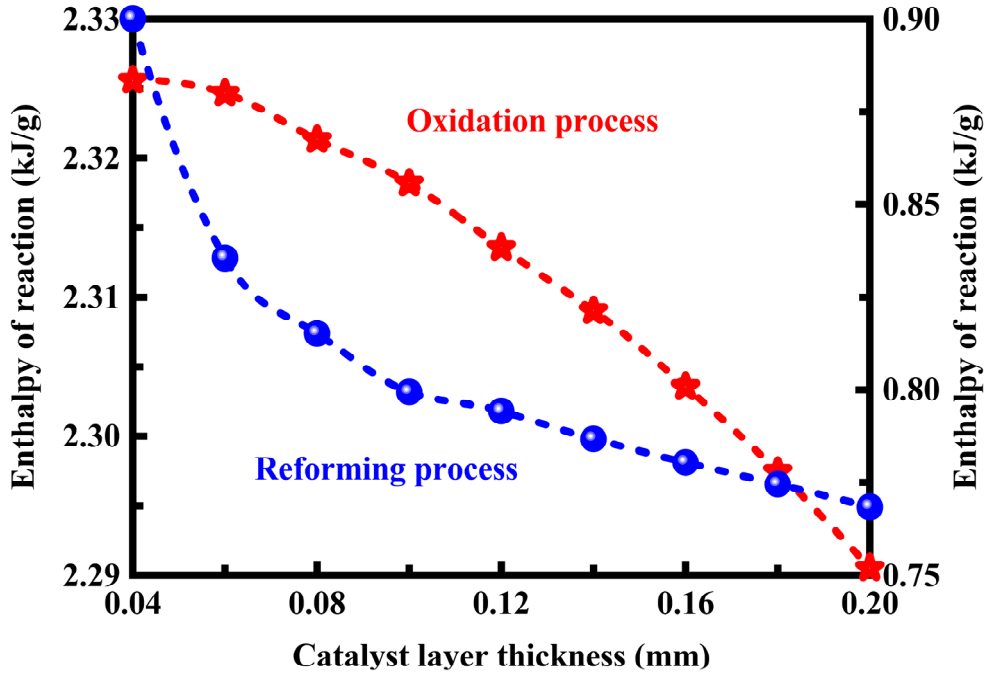

Figure 3. Effect of catalyst layer thickness on the enthalpy of reaction in the oxidation and reforming processes of the thermally coupled reactor for conducting simultaneous endothermic and exothermic reactions.

The effect of catalyst layer thickness on the methanol conversion and hydrogen yield in the oxidation and reforming processes is illustrated in Figure 4 in the thermally coupled reactor for conducting simultaneous endothermic and exothermic reactions. In addition to the reaction channels, additional features such as microchannel or non-microchannel heat exchangers may be present. Microchannel heat exchangers are preferred. Adjacent heat transfer microchannels enable temperature in the reaction channel to be controlled precisely to promote steam reforming and minimize unselective reactions in the gas phase. The thickness of a wall between adjacent process channels and heat exchange channels is preferably 0.80 mm or less. Each of the process or heat exchange channels may be further subdivided with parallel subchannels. The heat exchange fluids can be gases or liquids and may include steam, liquid metals, or any other known heat exchange fluids. Especially preferred heat exchangers include combustors in which a fuel is oxidized to produce heat for the steam reforming reaction. The incorporation of a simultaneous exothermic reaction to provide an improved heat source can provide a typical heat flux of roughly an order of magnitude above the convective cooling heat flux. The flow of hot fluid through a heat exchanger may be cross flow, counter-flow or co-flow. For all of the above conditions, the approach to equilibrium conversion is the ratio of measured hydrocarbon conversion to equilibrium hydrocarbon conversion. The equilibrium composition or moles hydrocarbon out at equilibrium is based upon the measured average pressure of the inlet and outlet of the reactor zone and the inlet molar composition. The equilibrium distribution or composition for a given

temperature, pressure, and inlet mole fraction distribution can be calculated using Gibbs free energies with programs. The catalyst requires catalytically active surface sites that reduce the kinetic barrier to the steam reforming reaction. The catalyst comprises one or more of the following catalytically active materials: ruthenium, rhodium, iridium, nickel, palladium, platinum, and carbide of group VIB. Rhodium is particularly preferred. The catalytically active materials are typically quite expensive. Therefore, it is desirable to minimize the amount used to accomplish the desired performance. The catalyst also contains an alumina support for the catalytically active materials. An alumina support contains aluminum atoms bonded to oxygen atoms, and additional elements can be present. Preferably, the alumina support comprises stabilizing element or elements that improve the stability of the catalyst in hydrothermal conditions. Stabilizing elements typically are large, highly charged cations. Preferably, the catalytically active materials are present in the form of small particles on the surface of the stabilized alumina support. The catalytically active layer is preferably disposed on a porous substrate. Preferably, the catalyst contains an alumina layer disposed on a thermally conductive surface. The surface could be, for example, a porous substrate or reaction chamber walls.

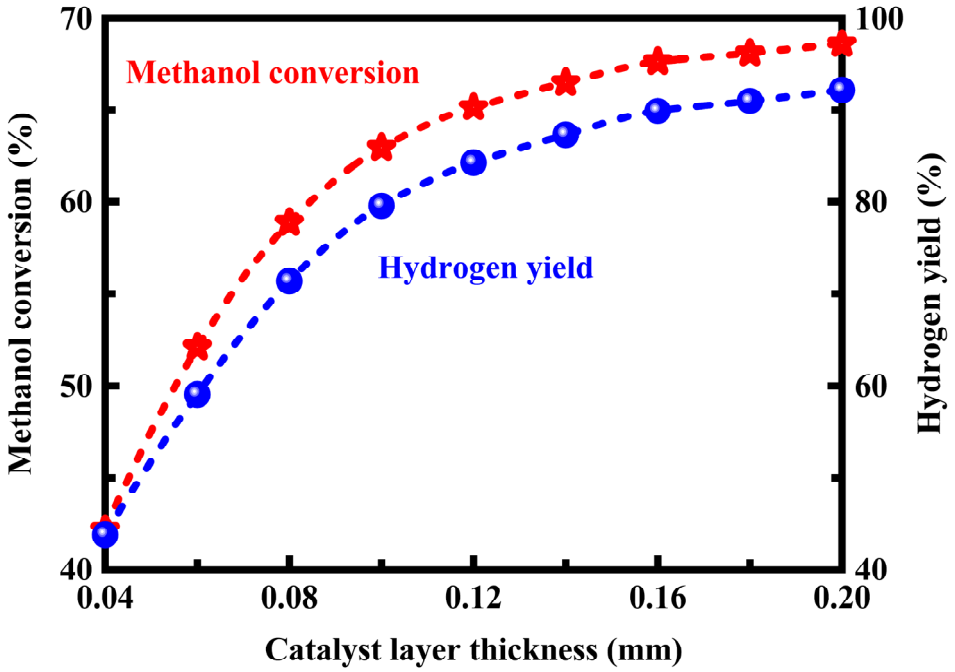

Figure 4. Effect of catalyst layer thickness on the methanol conversion and hydrogen yield in the oxidation and reforming processes of the thermally coupled reactor for conducting simultaneous endothermic and exothermic reactions.

The methanol and oxygen mole fraction contour plots are illustrated in Figure 5 in the thermally coupled reactor for conducting simultaneous endothermic and exothermic reactions. In a steam reforming process, a mixture of a hydrocarbon feedstock and steam, and in some cases also carbon dioxide or other components, is passed at an elevated pressure through particulate catalyst-filled heat exchange tubes, which are externally heated by means of a suitable heating medium, generally a hot gas mixture [51, 52]. The catalyst is normally in the form of shaped units, for example, cylinders having a plurality of through holes, and is typically formed from a refractory support material, for example, alumina, impregnated with a suitable catalytically active metal such as nickel [53, 54]. Structured steam reforming catalysts offer higher heat transfer, higher activity and lower pressure drop than particulate steam reforming catalysts. Therefore, there have been proposals to use them throughout the entire depth of the tube to maximize the performance of the steam reformer in terms of obtaining the lowest tube wall temperature, the lowest pressure drop and the maximum hydrocarbon conversion [55, 56]. Structured steam reforming catalysts however are typically manufactured from metals,

typically high temperature alloys [57, 58]. The strength of these materials reduces substantially at the temperatures encountered at the outlet of steam reformers. Therefore, as the structured catalyst is often formed from leaves of very thin material with little weight bearing capability, it is often mounted on a central core structure that supports all of the weight of the catalyst along with the imposed pressure drop load. Structured catalysts offer heat transfer benefits and extra activity, which is more effective in the inlet zone of the steam reformer. However, in the outlet zone of the steam reformers where the duty is lower, the structured catalyst may be replaced with a conventional particulate catalyst to provide the desired conversion at an overall lower cost than if structured catalysts were used along the entire length of the tubes. Another key benefit of the present arrangement is that it overcomes the need for extensive support structures often required for structured catalysts, in particular at the at the bottom of the tubes due to high temperature, total weight and pressure drop. Furthermore, loading and unloading of the structured catalyst may be shortened and the flexibility to provide tailored reforming solutions improved. Therefore, using structured catalyst at the inlet of the tubes and particulate catalyst at the outlet of the tubes offers a more cost effective and more robust catalyst arrangement than particulate catalyst alone, structured catalyst alone or alternative arrangements of particulate catalyst and structured catalyst. The steam reformer contains a plurality of vertical tubes through which the gas mixture may be passed, and to which heat is transferred by means of a hot gas flowing around the tubes. The tube inlets are typically at the top end such that the feed gas mixture is typically fed to the top of the steam reformer and flows downward through the tubes. The steam reforming reactions are endothermic and heat is transferred to the tubes by means of a hot gas flowing around the exterior surfaces of the tubes. Various steam reformer arrangements may be used. Consequently, the steam reformer may be a conventional top-fired steam reformer or a side-fired steam reformer. In such reformers the hot gas is provided by combusting a fuel gas using a plurality of burners disposed either at the top end or along the length of the tubes. Alternatively, the steam reformer may be a gas-heated reformer in which the hot gas may be provided by a flue-gas from a combustion process, or may be a gas generated by catalytic or non-catalytic partial oxidation of a hydrocarbon, or by autothermal reforming of a hydrocarbon and the reformed gas mixture. Furthermore, the hot gas may be mixed with the reformed gas that has passed through the plurality of tubes.

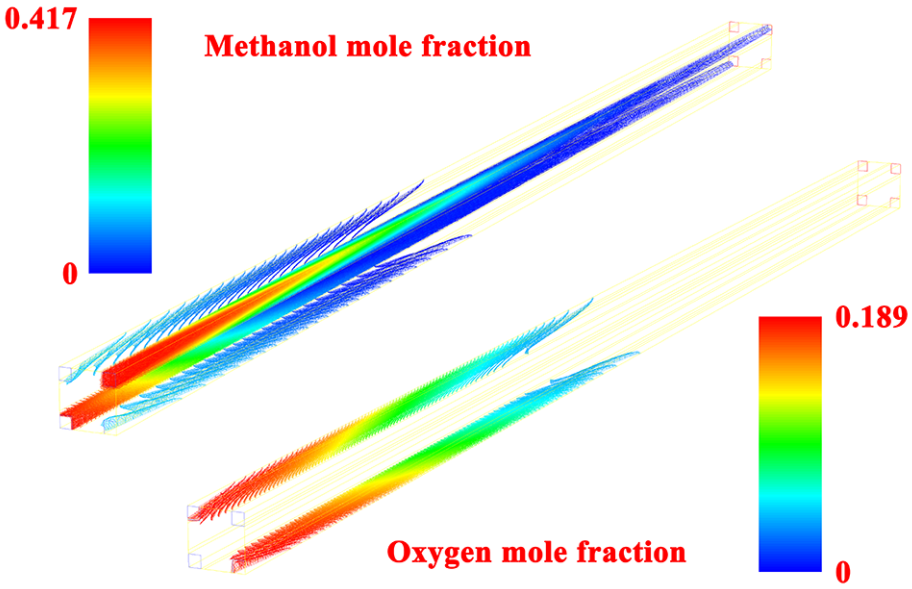

Figure 5. Methanol and oxygen mole fraction contour plots in the thermally coupled reactor for conducting simultaneous endothermic and exothermic reactions.

The chemical enthalpy and sensible enthalpy contour plots are illustrated in Figure 6 in the thermally coupled reactor for conducting simultaneous endothermic and exothermic reactions. A thin

layer of a slurry containing the ceramic precursor is applied on the surface by means of spraying, painting, or dipping. After applying for the coat, the slurry is dried and calcined at a temperature usually in the region of 350-1000 °C. Finally, the ceramic layer is impregnated with the catalytic active material. Alternatively, the catalytic active material is applied for simultaneously with the ceramic precursor. Unfortunately, a number of disadvantages of the catalyzed hardware reactors compared to fixed bed reactors exists. The catalyst layer cannot be replaced if it loses its activity either by ageing or by poisoning. The catalytic layer can only be applied to certain materials. The reactor tubes have to be made of this type of material which may be more expensive than a conventional tube material. The steam reforming reactions occurs under pressurized conditions and the tube thickness is large, hence the cost of materials influences the price significantly. Furthermore, production of long catalyzed hardware reactor tubes can be difficult. The reactor tube can have a length of 50 mm or more. It will be difficult to obtain an even thickness of the reforming catalyst layer throughout such a length, and means to obtain an even layer, which can be used for small scale application such as centrifuging the tube, is more difficult to apply for this size of tubes. Additionally, appropriate heat treatment of a tube of this size can be difficult. These drawbacks can be overcome by producing the catalyzed hardware separately from the reactor. A metal support is cut into an appropriate size. The sheet is wash-coated. After the wash-coating, the sheet is formed into the appropriate shape. Alternatively, the sheet is formed into the final shape prior to the wash-coating. The metallic support is formed substantially to have the same shape as the reactor wall and is arranged in a direct heat conduction relationship with the reactor wall. It will be possible to change the catalytic layer if it no longer has sufficient catalytic activity. The expensive steel used to obtain adhesion of the catalyst to the metal surface will only comprise a small fraction of the total metal consumption. The catalyzed hardware can be produced in smaller sections, which will be easier to manufacture and handle. Pressure drop in the catalyzed reformer tube is much lower than in the conventional case for the same tube diameter. This enables the use of reactor tubes with a smaller diameter and still maintaining an acceptable pressure drop. Smaller tube diameter results in an increased tube lifetime, tolerates higher temperatures and reduces the tube material consumption.

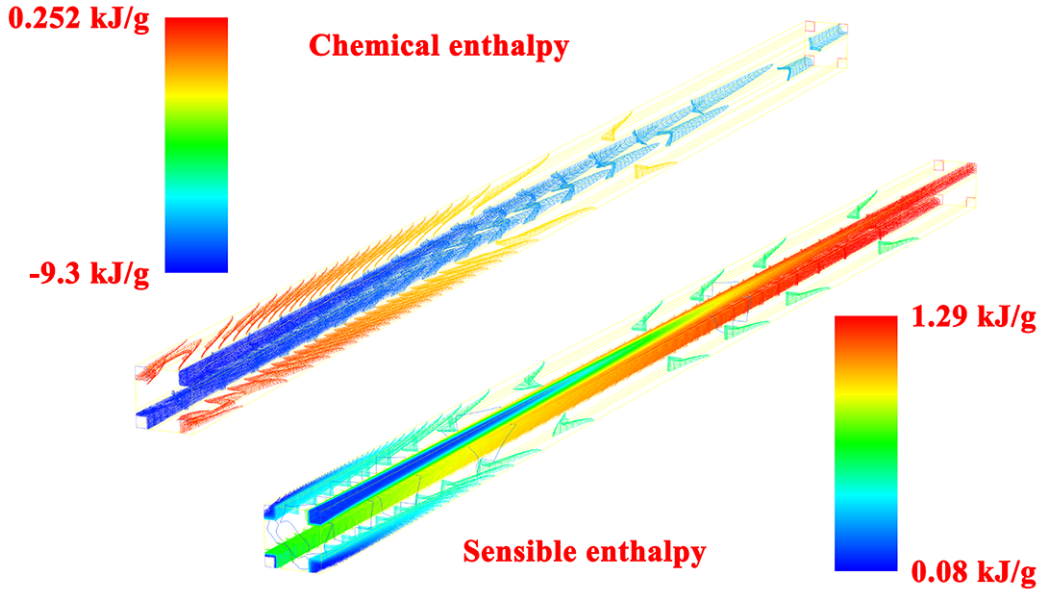

Figure 6. Chemical enthalpy and sensible enthalpy contour plots in the thermally coupled reactor for conducting simultaneous endothermic and exothermic reactions.

The oxidation reaction rate profiles are presented in Figure 7 along the length of the thermally coupled reactor for conducting simultaneous endothermic and exothermic reactions. In top-fired or side-fired reformers, the burners are typically fed with a fuel gas mixture comprising a hydrocarbon, such as methane, and which may further comprise hydrogen or other suitable fuel gases. Combustion is

performed using an oxidant such as air, which is also fed to the one or more burners to form the hot combustion gas. In the case of a top-fired reformer the inlets for the feed gas mixture are typically located at the top end of the reformer and the outlets for the reformed gas mixture at the bottom end [59, 60]. The burners are located at the top end and the combusted gas outlet is typically located at the bottom end [61, 62]. In the case of a side-fired reformer the inlets for the feed gas mixture are typically located at the top end of the reformer and the outlets for the reformed gas mixture at the bottom end [63, 64]. The burners in this case are located at multiple levels between the top end and the bottom end and the combusted gas outlet is typically located at the top end [65, 66]. The feed gas mixture may be passed to distribution means, such as header pipes which distribute the feed gas mixture to the heat exchange tubes. The tubes pass through a heat exchange zone in which heat is transferred to the reactants passing through the tubes. Collector pipes may be connected to the bottom of the tubes, which provide channels for collection of the reformed gas. Such distribution and collection means define an inlet zone and an outlet zone above and below the heat exchange zone. They may be termed boundary means as they define boundaries between the heat exchange zone and the inlet and outlet zones. In gas-heated reformers, the inlet for the feed gas mixture is typically located at the top end of the reformer. The feed gas mixture may be passed to distribution means, such as header pipes which distribute the feed gas mixture to the heat exchange tubes. The tubes pass through a heat exchange zone in which heat is transferred to the reactants passing through the tubes. Collector pipes may be connected to the bottom of the tubes and the reformed gas outlet which may be at the bottom end of the steam reformer. Alternatively, tube-sheets may be provided to separate the inlet and outlet zones from the heat exchange zone. Consequently, a tube-sheet may separate the heat exchange zone through which the hot gas passes from a zone, such as a plenum chamber, communicating with the interior of the heat exchange tubes to permit feed of feed gas mixture to the tubes or off-take of reformed gas from the tubes. Alternatively, there may be a combination of tube-sheets and header pipes. Alternatively, the heat exchange tubes may discharge the reformed gas into the heat exchange zone containing the hot gas to form a reformed gas mixture which is recovered from the reformed gas outlet. The reformed gas may be recovered from the top end or bottom end of the steam reformer. Again, the tube-sheets or header or collector may be termed boundary means as they define boundaries between the heat exchange zone and the inlet and outlet zones. Preferably hot gas distribution means, such as baffles, are provided within the reformer that causes the hot gas to flow evenly through the reformer. Desirably all of the tubes contain the same proportions of structured catalyst and particulate catalyst, although this is not essential. This provides the benefits of the higher activity, higher heat transfer, and low pressure drop of the structured catalyst at the inlet end and the benefit of the cheaper and stronger particulate catalyst at the outlet end. Each tube has an inlet for the feed gas mixture, an outlet for the reformed gas mixture, and the tubes contain a particulate steam reforming catalyst adjacent the outlet and a structured steam reforming catalyst adjacent the inlet, so that the feed gas mixture contacts the structured steam reforming catalyst and then the particulate steam reforming catalyst. In the case of a methanol steam reformer, where feed stream contains water and methanol, these components may be mixed together and delivered as a single stream. Alternatively, these components may be separately delivered to the reforming region. Although the reformate stream contains a substantial amount of hydrogen gas, the stream may also be referred to as a mixed gas stream because it also contains gases other than hydrogen gas. Examples of these gases include carbon dioxide, carbon monoxide, water, methane and unreacted methanol or other carbon-containing feedstocks. A feed stream may be delivered to the steam reformer at an elevated temperature, and accordingly may provide at least a portion of the required heat. When a burner or other combustion chamber is used, a fuel stream is consumed and a heated exhaust stream is produced. The feed stream is vaporized prior to undergoing the reforming reaction, and the heating assembly may be adapted to heat and vaporize any liquid components of the feed stream.

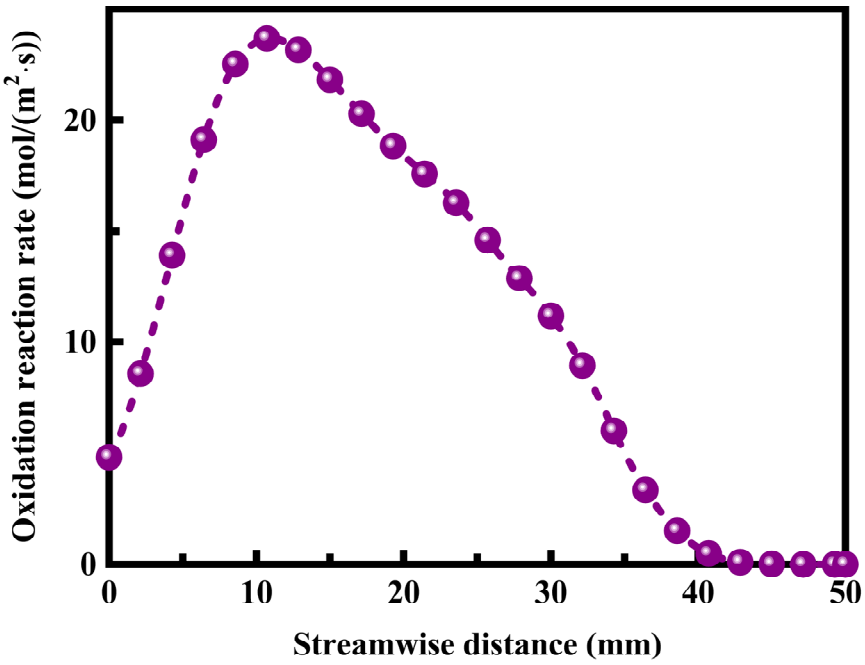

Figure 7. Oxidation reaction rate profiles along the length of the thermally coupled reactor for conducting simultaneous endothermic and exothermic reactions.

The reforming reaction rate profiles are presented in Figure 8 along the length of the thermally coupled reactor for conducting simultaneous endothermic and exothermic reactions. This steam reforming reaction is carried out using, as raw materials, methanol and steam fed into the ceramic tubular reactors so as to yield a reformed gas containing hydrogen and carbon dioxide. In such a steam reforming reaction, methanol is reacted with steam while the reforming material containing the methanol and steam is heated with part of combustion heat so as to yield a reformed gas containing hydrogen and carbon dioxide. In a low-temperature region where the reactivity is low, a steam reforming reaction is carried out by the catalysis of a reforming catalyst. The term catalyzed hardware is used for a catalyst system where a layer of catalyst is fixed on a surface of another material, for example, metallic surfaces. The other material serves as the supporting structure giving strength to the system. This allows to design catalyst shapes which would not have sufficient mechanical strength in itself. The steam reforming technology makes use of reforming catalyst in the form of pellets of various sizes and shapes. The catalyst pellets are placed in fixed bed reactors. The reforming reaction is endothermic. In conventional reformers, the necessary heat for the reaction is supplied from the environment outside the tubes usually by a combination of radiation and convection to the outer side of the reformer tube. The heat is transferred to the inner side of the tube by heat conduction through the tube wall and is transferred to the gas phase by convection. Finally, the heat is transferred from the gas phase to the catalyst pellet by convection. The catalyst temperature can be more than 80 °C lower than the inner tube wall temperature at the same axial position of the reformer tube. Heat transport is more efficient when catalyzed hardware is used in the steam reforming process. The heat transport to the catalyst occurs by conduction from the inner tube wall. This is a much more efficient transport mechanism than the transport by convection via the gas phase. The result is that the temperatures of the inner tube wall and the catalyst are almost identical. Furthermore, the tube thickness can be reduced, which makes the temperature difference between the inner and outer side of the reformer tube smaller. It is hence possible to have both a higher catalyst temperature and a lower tube temperature, all other conditions being the same when replacing the conventional reformer tubes with catalyzed hardware tubes. A low outer tube wall temperature is desirable since it prolongs the lifetime of the tube. A high catalyst temperature is advantageous since the reaction rate increases with temperature and since the equilibrium of reaction is shifted to the right-hand side resulting in a better utilization of the feed.

Finally, the catalyst amount is reduced when using catalyzed hardware reformer tubes compared to the conventional reformer with a fixed bed of reforming catalyst. The critical steam to carbon ratio decreases when the operating pressure is increased. The operating pressure in the thermally coupled reactor is the critical parameter for suppressing soot formation. By increasing the operating pressure, it is possible to operate advantageously at a lower steam to carbon ratio. The actual critical pressure will depend on the burner design used in the thermally coupled reactor.

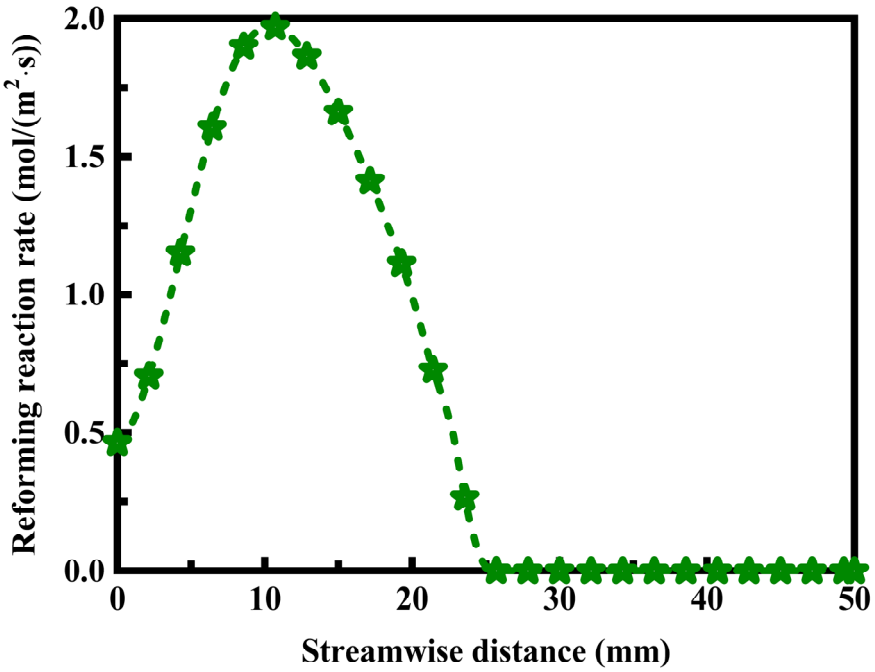

Figure 8. Reforming reaction rate profiles along the length of the thermally coupled reactor for conducting simultaneous endothermic and exothermic reactions.

4. Conclusions

Computational fluid dynamics simulations are carried out to better understand how to manage thermally coupled reactors for conducting simultaneous endothermic and exothermic reactions. Particular emphasis is placed upon the mechanisms involved in the heat transfer processes in thermally coupled reactors for hydrogen production by steam reforming. The effects of catalyst layer thickness on the enthalpy of reaction, methanol conversion, and hydrogen yield are delineated. The oxidation and reforming reaction rates involved in the endothermic and exothermic processes are determined. Contour maps denoting temperature, enthalpy, and species mole fractions are constructed and design recommendations are made. The major conclusions are summarized as follows:

- The waste heat can efficiently be recovered in a low-temperature region, although the reactivity of a steam reforming reaction is low in such a region.
- The steam reforming device is configured as to be heated by part of the combustion heat to cause a steam reforming reaction in the device.
- The steam reforming reaction is endothermic and is therefore typically carried out in an externally heated steam reforming reactor.
- The incorporation of a simultaneous exothermic reaction to provide an improved heat source can provide a typical heat flux of roughly an order of magnitude above the convective heat flux.
- Structured catalysts offer heat transfer benefits and extra activity, which is more effective in the inlet zone of the steam reformer.
- The metallic support is formed substantially to have the same shape as the reactor wall and is arranged in a direct heat conduction relationship with the reactor wall.

- Desirably all of the tubes contain the same proportions of structured catalyst and particulate catalyst, which provides the benefits of the higher activity, higher heat transfer, and low pressure drop of the structured catalyst at the inlet end and the benefit of the stronger particulate catalyst at the outlet end.
- Heat transport is more efficient when catalyzed hardware is used in the steam reforming process.

References

[1] F.P. Rigas. Chemical engineering kinetics of p-xylene chlorination in a gas-liquid agitated reactor. *Chemical Engineering Science*, Volume 265, 2023, Article Number: 118216.

[2] Y. Ammar, P. Cognet, and M. Cabassud. ANN for hybrid modelling of batch and fed-batch chemical reactors. Chemical Engineering Science, Volume 237, 2021, Article Number: 116522.

[3] J. Solsvik, T. Haug-Warberg, and H.A. Jakobsen. Implementation of chemical reaction equilibrium by Gibbs and Helmholtz energies in tubular reactor models: Application to the steam-methane reforming process. *Chemical Engineering Science*, Volume 140, 2016, Pages 261-278.

[4] M. Miyamoto, C. Hayakawa, K. Kamata, M. Arakawa, and S. Uemiya. Influence of the pre-reformer in steam reforming of dodecane using a Pd alloy membrane reactor. *International Journal of Hydrogen Energy*, Volume 36, Issue 13, 2011, Pages 7771-7775.

[5] G. Fernholz, S. Engell, L.-U. Kreul, and A. Gorak. Optimal operation of a semi-batch reactive distillation column. *Computers & Chemical Engineering*, Volume 24, Issues 2-7, 2000, Pages 1569-1575.

[6] K.S. Knaebel and F.B. Hill. Pressure swing adsorption: Development of an equilibrium theory for gas separations. *Chemical Engineering Science*, Volume 40, Issue 12, 1985, Pages 2351-2360.

[7] M. Seiiedhoseiny, K. Ghasemzadeh, E. Jalilnejad, and A. Iulianelli. Computational fluid dynamics study on concentration polarization phenomena in silica membrane reactor during methanol steam reforming. *Chemical Engineering and Processing - Process Intensification*, Volume 183, 2023, Article Number: 109249.

[8] H.C. Yoon, J. Otero, and P.A. Erickson. Reactor design limitations for the steam reforming of methanol. *Applied Catalysis B: Environmental*, Volume 75, Issues 3-4, 2007, Pages 264-271.

[9] A.M. Toikka and J.D. Jenkins. Conditions of thermodynamic equilibrium and stability as a basis for the practical calculation of vapour-liquid equilibria. *Chemical Engineering Journal*, Volume 89, Issues 1-3, 2002, Pages 1-27.

[10] J. Mitrovic. Upon equilibrium of gas bubble in infinite liquid. *Chemical Engineering Science*, Volume 55, Issue 12, 2000, Pages 2265-2270.

[11] W. Nicol, D. Hildebrandt, and D. Glasser. The cost of crossing reaction equilibrium in a system that is overall adiabatic. *Computers & Chemical Engineering*, Volume 26, Issue 6, 2002, Pages 803-809.

[12] M. Castier, R.O. Espósito, F.W. Tavares, and R.P. Peçanha. Calculation of sedimentation equilibrium using a modified flash algorithm. *Chemical Engineering Science*, Volume 56, Issue 12, 2001, Pages 3771-3779.

[13] E.V. Kustova, E.A. Nagnibeda, and A. Chikhaoui. On the accuracy of non-equilibrium transport coefficients calculation. *Chemical Physics*, Volume 270, Issue 3, 2001, Pages 459-469.

[14] J.G.M. Winkelman, O.K. Voorwinde, M. Ottens, A.A.C.M. Beenackers, and L.P.B.M. Janssen. Kinetics and chemical equilibrium of the hydration of formaldehyde. *Chemical Engineering Science*, Volume 57, Issue 19, 2002, Pages 4067-4076.

[15] A.K. Dutt. Equilibrium and nonequilibrium steady states in the reversible Oregonator model. *Chemical Physics*, Volume 162, Issues 2-3, 1992, Pages 265-270.

[16] J.K. Ali, E.J. Newson, and D.W.T. Rippin. Exceeding equilibrium conversion with a catalytic membrane reactor for the dehydrogenation of methylcyclohexane. *Chemical Engineering Science*, Volume 49, Issue 13, 1994, Pages 2129-2134.
[17] I. Rips. Nonadiabatic reactions in condensed phase in the absence of thermal equilibrium. *Chemical Physics*, Volume 235, Issues 1-3, 1998, Pages 243-255.
[18] A. Lucia, L. Padmanabhan, and S. Venkataraman. Multiphase equilibrium flash calculations. *Computers & Chemical Engineering*, Volume 24, Issue 12, 2000, Pages 2557-2569.
[19] F.J.L. Castillo, and G.P. Towler. Application of linearised vapour-liquid equilibrium equations. *Chemical Engineering Science*, Volume 52, Issue 19, 1997, Pages 3405-3407.
[20] A. Jamnik. Sedimentation equilibrium of adhesive spheres in a planar gap. *Chemical Physics Letters*, Volume 292, Issues 4-6, 1998, Pages 481-486.
[21] O.J. Bricio, J. Coca, and H. Sastre. Modelling equilibrium isotherms for styrene-divinylbenzene ion exchange resins. *Chemical Engineering Science*, Volume 53, Issue 7, 1998, Pages 1465-1467.
[22] H. Segura and J. Wisniak. Influence of excess properties on binary liquid-liquid equilibrium. *Chemical Engineering Science*, Volume 52, Issue 4, 1997, Pages 597-610.
[23] J. Piotrowski, R. Kozak, and M. Kujawska. Thermodynamic model of chemical and phase equilibrium in the urea synthesis process. *Chemical Engineering Science*, Volume 53, Issue 1, 1998, Pages 183-186.
[24] F. Jalali and J.D. Seader. Homotopy continuation method in multi-phase multi-reaction equilibrium systems. *Computers & Chemical Engineering*, Volume 23, Issue 9, 1999, Pages 1319-1331.
[25] H.I. Moe, S. Hauan, K.M. Lien, and T. Hertzberg. Dynamic model of a system with phase- and reaction equilibrium. *Computers & Chemical Engineering*, Volume 19, Supplement 1, 1995, Pages 513-518.
[26] S. Ung and M.F. Doherty. Vapor-liquid phase equilibrium in systems with multiple chemical reactions. *Chemical Engineering Science*, Volume 50, Issue 1, 1995, Pages 23-48.
[27] D. Barbosa and M.F. Doherty. The influence of equilibrium chemical reactions on vapor-liquid phase diagrams. *Chemical Engineering Science*, Volume 43, Issue 3, 1988, Pages 529-540.
[28] A. Seidel. Calculating chemical reaction equilibrium for a homogeneous phase from the material balance of a batch reactor. *Chemical Engineering Science*, Volume 45, Issue 9, 1990, Pages 2970-2973.
[29] R. Cabello, A.E.P. Popescu, J. Bonet-Ruiz, D.C. Cantarell, and J. Llorens. Heat transfer in pipes with twisted tapes: CFD simulations and validation. *Computers & Chemical Engineering*, Volume 166, 2022, Article Number: 107971.
[30] E.M. Moghaddam, E.A. Foumeny, A.I. Stankiewicz, and J.T. Padding. Multiscale modelling of wall-to-bed heat transfer in fixed beds with non-spherical pellets: From particle-resolved CFD to pseudo-homogenous models. *Chemical Engineering Science*, Volume 236, 2021, Article Number: 116532.
[31] O.P. Klenov, N.A. Chumakova, S.A. Pokrovskaya, and A.S. Noskov. Impact of heat and mass transfer in porous catalytic monolith: CFD modeling of exothermic reaction. *Chemical Engineering Science*, Volume 205, 2019, Pages 1-13.
[32] D. Taler and P. Ocłoń. Determination of heat transfer formulas for gas flow in fin-and-tube heat exchanger with oval tubes using CFD simulations. *Chemical Engineering and Processing: Process Intensification*, Volume 83, 2014, Pages 1-11.
[33] S. Lopatin, A. Elyshev, and A. Zagoruiko. CFD modeling of the structured cartridges with glass-fiber catalysts. *Chemical Engineering Research and Design*, Volume 190, 2023, Pages 255-267.
[34] A. Amini, M.H. Sedaghat, S. Jamshidi, A. Shariati, and M.R. Rahimpour. A comprehensive CFD

simulation of an industrial-scale side-fired steam methane reformer to enhance hydrogen production. *Chemical Engineering and Processing - Process Intensification*, Volume 184, 2023, Article Number: 109269.

[35] V. Surendran, M. Bracconi, J.A.H. Lalinde, M. Maestri, and J. Kopyscinski. Assessment of a catalytic plate reactor with in-situ sampling capabilities by means of CFD modeling and experiments. *Chemical Engineering Journal*, Volume 446, Part 3, 2022, Article Number: 136999.

[36] M. Bracconi. CFD modeling of multiphase flows with detailed microkinetic description of the surface reactivity. *Chemical Engineering Research and Design*, Volume 179, 2022, Pages 564-579.

[37] A.A.G. Maia, D.F. Cavalca, J.T. Tomita, F.P. Costa, and C. Bringhenti. Evaluation of an effective and robust implicit time-integration numerical scheme for Navier-Stokes equations in a CFD solver for compressible flows. *Applied Mathematics and Computation*, Volume 413, 2022, Article Number: 126612.

[38] G.R. Whitehouse and A.H. Boschitsch. Investigation of grid-based vorticity-velocity large eddy simulation off-body solvers for application to overset CFD. *Computers & Fluids*, Volume 225, 2021, Article Number: 104978.

[39] M. Jadoui, C. Blondeau, E. Martin, F. Renac, and F.-X. Roux. Comparative study of inner-outer Krylov solvers for linear systems in structured and high-order unstructured CFD problems. *Computers & Fluids*, Volume 244, 2022, Article Number: 105575.

[40] L. Berenguer and D. Tromeur-Dervout. Developments on the Broyden procedure to solve nonlinear problems arising in CFD. *Computers & Fluids*, Volume 88, 2013, Pages 891-896.

[41] L. Berenguer and D. Tromeur-Dervout. Asynchronous partial update of the restricted additive schwarz preconditioner to solve nonlinear CFD problems. *Computers & Fluids*, Volume 110, 2015, Pages 211-218.

[42] G. Houzeaux, R.M. Badia, R. Borrell, D. Dosimont, J. Ejarque, M. Garcia-Gasulla, and V. López. Dynamic resource allocation for efficient parallel CFD simulations. *Computers & Fluids*, Volume 245, 2022, Article Number: 105577.

[43] V. Kovenya, S. Cherny, S. Sharov, V. Karamyshev, and A. Lebedev. On some approaches to solve CFD problems. *Computers & Fluids*, Volume 30, Issues 7-8, 2001, Pages 903-916.

[44] J. Sahu and K.R. Heavey. Parallel CFD computations of projectile aerodynamics with a flow control mechanism. *Computers & Fluids*, Volume 88, 2013, Pages 678-687.

[45] D. Jones, J.-D. Müller, and F. Christakopoulos. Preparation and assembly of discrete adjoint CFD codes. *Computers & Fluids*, Volume 46, Issue 1, 2011, Pages 282-286.

[46] E. Oktay, H.U. Akay, and O. Merttopcuoglu. Parallelized structural topology optimization and CFD coupling for design of aircraft wing structures. *Computers & Fluids*, Volume 49, Issue 1, 2011, Pages 141-145.

[47] S. Chakraborty and V. Balakotaiah. Low-dimensional models for describing mixing effects in laminar flow tubular reactors. *Chemical Engineering Science*, Volume 57, Issue 13, 2002, Pages 2545-2564.

[48] D.L. Marcfflsio, R.O. Fox, A.A. Barresi, M. Garbero, and G. Baldi. On the simulation of turbulent precipitation in a tubular reactor via computational fluid dynamics (CFD). *Chemical Engineering Research and Design*, Volume 79, Issue 8, 2001, Pages 998-1004.

[49] A. Baltsas, E. Papadopoulos, and C. Kiparissides. Application and validation of the pseudo-kinetic rate constant method to high pressure LDPE tubular reactors. *Computers & Chemical Engineering*, Volume 22, Supplement 1, 1998, Pages S95-S102.

[50] M. Berezowski, E.W. Jacobsen, and R. Grzywacz. Dynamics of heat-integrated heterogeneous tubular reactors with axial heat conductivity in reactor wall. *Computer Aided Chemical Engineering*, Volume 9, 2001, Pages 99-104.

[51] E. Meloni, M. Martino, A. Ricca, and V. Palma. Ultracompact methane steam reforming reactor based on microwaves susceptible structured catalysts for distributed hydrogen production. *International Journal of Hydrogen Energy*, Volume 46, Issue 26, 2021, Pages 13729-13747.

[52] V. Palma, M. Martino, E. Meloni, and A. Ricca. Novel structured catalysts configuration for intensification of steam reforming of methane. *International Journal of Hydrogen Energy*, Volume 42, Issue 3, 2017, Pages 1629-1638.

[53] C. Fukuhara and K. Kawamorita. A structured catalyst: Noble metal supported on a plate-type zirconia substrate prepared by anodic oxidation for steam reforming of hydrocarbon. *Applied Catalysis A: General*, Volume 370, Issues 1-2, 2009, Pages 42-49.

[54] V. Palma, A. Ricca, E. Meloni, M. Martino, M. Miccio, and P. Ciambelli. Experimental and numerical investigations on structured catalysts for methane steam reforming intensification. *Journal of Cleaner Production*, Volume 111, Part A, 2016, Pages 217-230.

[55] H.C. Lee, Y. Potapova, and D. Lee. A core-shell structured, metal-ceramic composite-supported Ru catalyst for methane steam reforming. *Journal of Power Sources*, Volume 216, 2012, Pages 256-260.

[56] E. López, N.J. Divins, A. Anzola, S. Schbib, D. Borio, and J. Llorca. Ethanol steam reforming for hydrogen generation over structured catalysts. *International Journal of Hydrogen Energy*, Volume 38, Issue 11, 2013, Pages 4418-4428.

[57] S. Hull and J. Trawczyński. Steam reforming of ethanol on zinc containing catalysts with spinel structure. *International Journal of Hydrogen Energy*, Volume 39, Issue 9, 2014, Pages 4259-4265.

[58] A. Vita, L. Pino, F. Cipitì, M. Laganà, and V. Recupero. Structured reactors as alternative to pellets catalyst for propane oxidative steam reforming. *International Journal of Hydrogen Energy*, Volume 35, Issue 18, 2010, Pages 9810-9817.

[59] N.C.J.T. Richardson. Steam reforming of chlorocarbons: Chlorinated aromatics. *Applied Catalysis B: Environmental*, Volume 26, Issue 3, 2000, Pages 217-226.

[60] J. Cunha and J.L.T. Azevedo. Modelling the integration of a compact plate steam reformer in a fuel cell system. *Journal of Power Sources*, Volume 86, Issues 1-2, 2000, Pages 515-522.

[61] D.L. Trimm. Catalysts for the control of coking during steam reforming. *Catalysis Today*, Volume 49, Issues 1-3, 1999, Pages 3-10.

[62] D. Duprez. Selective steam reforming of aromatic compounds on metal catalysts. *Applied Catalysis A: General*, Volume 82, Issue 2, 1992, Pages 111-157.

[63] W. Wiese, B. Emonts, and R. Peters. Methanol steam reforming in a fuel cell drive system. *Journal of Power Sources*, Volume 84, Issue 2, 1999, Pages 187-193.

[64] Z. Zhang and M. Baerns. Hydrogen formation by steam-reforming and water-gas shift reaction in the oxidative methane coupling reaction over calcium oxide-cerium dioxide catalysts. *Applied Catalysis*, Volume 75, Issue 1, 1991, Pages 299-310.

[65] A.M. Meziou, P.B. Deshpande, and I.M. Alatiqi. Dynamic matrix control of an industrial steam gas reformer. *International Journal of Hydrogen Energy*, Volume 20, Issue 3, 1995, Pages 187-192.

[66] H. Al-Qahtani. Investigation of synthesis gas production from methane bypartial oxidation over selected steam reforming commercial catalysts. *Studies in Surface Science and Catalysis*, Volume 100, 1996, Pages 437-446.